

# TOPOLOGIC ANALYSIS OF SAMPLES AND CAVITIES: A NEW TOOL FOR MORPHOLOGIC INSPECTION OF QUENCH SITE

S. Berry<sup>#</sup>, C. Antoine, A. Aspart, J.P. Charrier, M. Desmons, L. Margueritte,  
CEA-Saclay, 91191 Gif-sur-Yvette, France

## Abstract

It has been demonstrated recently that local magnetic field enhancement can originate from roughness (e.g. steps at grain boundaries) [1]. We are willing to investigate if the quench observed in superconducting niobium cavities can be related to such morphological defects. We therefore have to develop two kinds of tool.

1) A replica technique that allows to reproduce the internal surface of cavities (non destructive testing).

2) A morphological analysis tool. Classical roughness measurements are not adapted to determine local curvature radius.

This paper describes a new topological approach aiming at a better characterization of the surface morphology. This technique has been applied to niobium samples treated with different surface treatments. We also present the first results applied to replica taken from cavities at the quench site.

## INTRODUCTION

In the race toward higher accelerating gradients, the quench phenomenon is the main limitation to reach the theoretically expected 50 MV/m. The quench is a thermal or magnetic instability, resulting in the superconducting to normal state fast transition. The quench is suspected to originate from a temperature or magnetic field increase on a local defect. Up to now the quench origin is not clearly identified. We want to investigate if the roughness of the inner surface could be responsible for this thermal instability. This paper is divided into three parts: a presentation of the morphological characterization of a surface with a new topological approach, then investigations on cavities which shows for the first time the visualization of a morphological defect at the quench site, and last studies on samples submitted to various surface treatments.

## SURFACE MORPHOLOGY ANALYSIS

### Surface roughness measurements

Surface roughness acquisition was carried out with a profiler equipped with a motor for the  $x$ - $y$  displacements. We used different types of sensors (one of them: Perthener-Mahr, type: FRW750, amplitude: 250  $\mu\text{m}$ ,  $z$  resolution: 0.1  $\mu\text{m}$ ). The stylus has a diamond tip of 60°, and the contact strength is 0.1 g. The height detection is inductive.

The  $z$  resolution is 0.1  $\mu\text{m}$  because restricted by mechanics of the lateral displacement system; and  $x$ - $y$  resolution is 1  $\mu\text{m}$ , restricted by motor step.

This technique is also called “mechanical microscopy”.

### Classical roughness parameters

What is the best parameter to describe the Nb surface? Classical roughness parameters ( $R_b$ ,  $R_a$ ,  $\sigma$ ,  $S_k$ ,  $E_k$ ) appear not well adapted [2]. For instance, arithmetic ( $R_a$ ) or quadratic ( $R_q$  or  $\sigma$  or  $rms$ ) roughness can easily be measured by profilometry, but one has to keep in mind that this parameter does not characterize well a surface in term of electromagnetic behaviour. Indeed very different field enhancement can be found with profiles having the same  $R_a$ .

### Conformal equivalent structures model

We propose a topological approach for a better characterization of the surface morphology. The surface obtained by mechanical microscopy is transformed using a conformal mapping that retains the surface orientations [3].

This approach is based on a parameterized representation taking the spatial angularity of micro-facets ( $ABCD$ ) as a parameter.

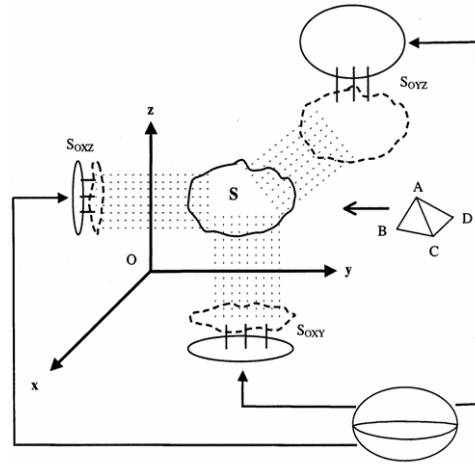


Figure 1: Analyzed surface projection and its ellipsoid projection on the three planes. In this analysis the analyzed surface is considered as composed of elementary micro-facets ( $ABCD$ ) from [3].

The result is an ellipsoid of developed surface equal to the developed surface of the analyzed area, but in which the connectivity has disappeared (see figure 1). The descriptive parameters of the ellipsoid ( $a$ ,  $b$ ,  $c$ , local radii of curvature, perimeter, section area ...) are used for a comparative study. Such topographic analysis is more accurate to describe the magnetic field enhancement [4].

<sup>#</sup>sberry@cea.fr

## CAVITIES

### *Temperature-mapping and quench locating*

Temperature mapping of quench revealed that the power dissipation causes localized losses in contrast to Q-slope which occurs throughout most of the cavity. The site of failure is located by high precision temperature mapping with 17 resistors rotating over the cavity surface  $\Delta_{res.} = 10 \text{ mm}$ ,  $\Delta_{angle} = 9.3 \text{ mm}$  [5].

After the RF test the cavity is set horizontally so that the welding seam at the quench longitude is the lowest point. Photographs of the inner surface are taken (see figure 2). The presence of a  $\varnothing 3 \text{ mm}$  ball helps to locate the precise longitude coordinate. The presence of the welding seam helps to locate the precise latitude coordinate.

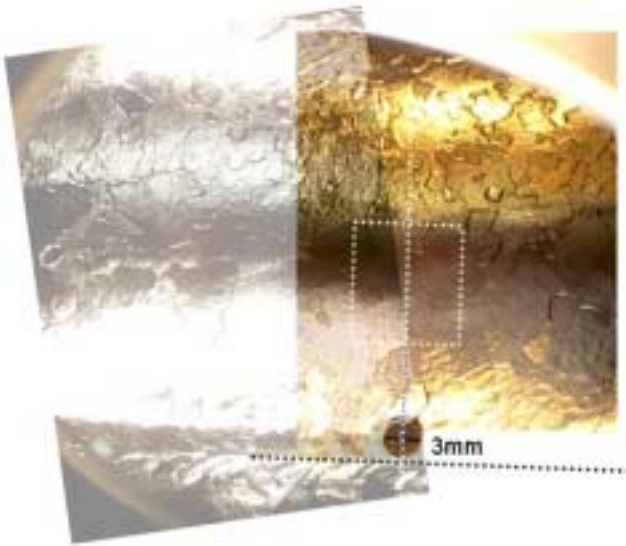


Figure 2: Picture of the inner surface with the hot area (white dotted line square) located thanks to the equator (black dotted line) and to the ball of 3 mm diameter.

### *Non destructive polymer replica technique*

The polymer replica technique is a non destructive replica method (resolution  $< 1 \mu\text{m}$ ). It consists of two steps:

- First making a negative replica of the inner surface with a siloxane polymer which polymerises within 15 min,
- Then replica of the inner surface with a bi-compound mixture of polyurethane held under 1-2 bar pressure for 15 min.

We have checked that replica technique followed by ultrasonic cleaning in  $65^\circ\text{C}$  basic bath leaves niobium surface free of polymer.

### *Surface morphology near welding seam*

We make several replicas on the inner surface near the equator. We observe a huge difference between the area of welding seam and a little farther away. The welding induces grain growth that leads to an important roughness

increase. Thus roughness measurement on samples gives only poor appreciation of the cavity surface morphology.

Never the less as will be shown hereafter, statistical comparison of surface morphology on samples might allow to classify different surface treatments.

Table 1:  $R_a$  parameters and  $c$  values from conformal ellipsoid representation for reference areas of annealed cavity polished with FNP mixture ( $10 \mu\text{m}$  step width, 600 steps square).

Parameter	out of welding seam	on welding seam
$R_a$ ( $\mu\text{m}$ )	$6.1 \pm 1.8$	$60.6 \pm 23.4$
$c$ ( $\mu\text{m}$ )	$96.5 \pm 3.6$	$354.3 \pm 7.2$

### *Surface morphology near the quench*

In this study we compare the surface morphology of the quench area and places far from the quench area. We have actually observed an insulated localized defect right in the middle of the hot spot (see figure 3).

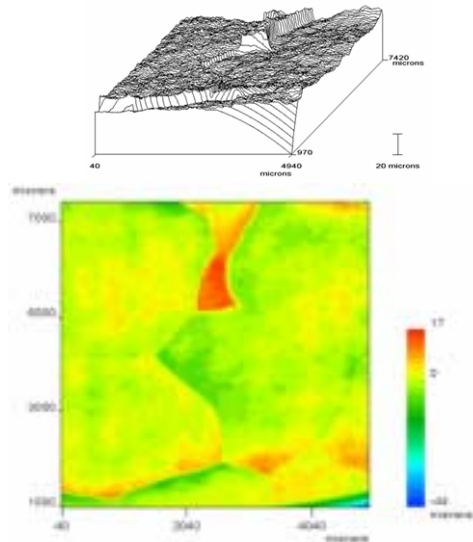


Figure 3: Quench area after a least mean square polynomial correction. A long and thin prominent grain perpendicular to magnetic field is observed. Top: 3D-view, bottom: contour lines.

### *Field enhancement factor calculation*

Numerical modelling of the field enhancement factor on the ridge of prominent grain is in progress and will be published elsewhere [6].

## SAMPLES

### *Sample preparation*

We want to compare various surface treatments in order to check if the conformal equivalent structure approach is relevant for our issue.  $100 \mu\text{m}$  were withdrawn. Nb samples cut from the same sheet were submitted to various surface treatments, and studied from the morphological point of view with surface profiler.

Three main factors have been explored at first:

- Annealed and not annealed samples are investigated. Optimized heat treatment with purification by Ti at 1300/1000°C [7].
- Surface treatments:
  - Electropolishing (EP): we have use the process now used at KEK, namely in a HF -H<sub>2</sub>SO<sub>4</sub> with the ratio 10%-90% in volume, with 10 Volts applied on the sample (as an anode).
  - Chemical polishing FNP: standard Chemical Polishing with HF, HNO<sub>3</sub> and H<sub>3</sub>PO<sub>4</sub> 1-1-2 in volume.
  - Chemical polishing FNS: Chemical Polishing with HF, HNO<sub>3</sub>, H<sub>2</sub>SO<sub>4</sub> 1-1-1 in volume.
- Different scales of observation and resolution (in each case the analyzed area is a square of 1024 steps):
  - at micron scale: “microroughness” 1 μm step width, the analyzed area is 1 mm<sup>2</sup>,

- at higher scale: “macroroughness” 10 μm step width, the analyzed area is 85 mm<sup>2</sup>.

Classical roughness parameters ( $R_b$ ,  $R_a$ ,  $\sigma$ ,  $S_k$ ,  $E_k$ ) as well as the ellipsoid parameters of the conformal ellipsoid representation ( $a$ ,  $b$ ,  $c$ ) are determined on each sample [8].

### Data analysis

#### General

- Measurements made in the same conditions on the same samples with two different facilities (LECA-Saclay and LMS-Besançon) give similar results.
- Roughness parameters as well as the ellipsoid parameters depend a lot on the scale of observation.
- Observation with a 9 μm step has a lower resolution but integrates ~10 times more grain boundaries. With a 1 μm step we get a better resolution and a better estimation of the micro-roughness on the surface of individual grains.

Table 2: Classical roughness parameters and  $a$ ,  $b$  and  $c$  values from conformal ellipsoid representation. Any change in the observation scale produces different results. Thus for quantitative comparison, we need to reproduce carefully the same conditions (explored area, step width, planarity, resolution...).

Surf. treat.		FNS	FNP	EP		FNS	FNP	EP
R <sub>t</sub> (μm)	9 μm annealed	312	46	14	9 μm not annealed	77	28	69,6
R <sub>a</sub> (μm)		38	5	0,8		9,4	1,9	4.33
σ (μm)		49,5	6,5	1,2		11,5	2,6	5.49
S <sub>k</sub>		-1,1	0,5	0,4		-0,07	0,02	-0,74
E <sub>k</sub>		4,2	3,4	4,8		2,7	3,8	3,95
Dev. Surf. (%)		101,36	100,1	100,05		100,3	100,64	100,1
a (μm)		3703	4566	3693		3833	3706	3907
b (μm)		3642	2954	3653		3519	3640	3452
c (μm)		314	98	63,2		185,4	313	78,5
Surf. treat.		1 μm annealed	FNS	FNP		EP	1 μm not annealed	FNS
R <sub>t</sub> (μm)	25,7		17,6	6,4	31,5	22,7		8.6
R <sub>a</sub> (μm)	2,8		2,9	0,69	4,8	2,2		0,8
σ (μm)	3,7		3,5	0,89	5,8	2,86		1,05
S <sub>k</sub>	0,7		0,08	-0,3	-0,4	0,1		-1.43
E <sub>k</sub>	4,4		2,4	4,8	3,5	3,4		5.70
Dev. Surf. (%)	100,19		100,13	100,05	100,08	101,77		100,1
a (μm)	482		424	408	550	540		431
b (μm)	345		393	408	303	309		386
c (μm)	15		12,1	9,3	35,7	49		13

#### Classical roughness parameters

- Preferential grain boundaries etching and/or etching pits can be inferred from  $S_k < 0$ .
- $E_k$  is  $> 3$  most of the time, this means that the repartition of morphologic defects is larger than a

*Gaussian one.* EP exhibits always the highest  $E_k$ , which means that there are a lot of “extreme” points (etching pits).

- Whatever scale, FNS exhibit the highest roughness while EP gives the smallest values. FNP, the usual BCP gives intermediate values.
- Samples with large grains (annealed) exhibit a very large dispersion in the macro-roughness (many grains studied). This arises from the large distribution in grain sizes, and thus in surface states.
- The main component of macro-roughness arises from the grain boundaries in the case of BCP. In the case of EP, where grain boundaries are only slightly etched, it arises mainly from etching pits.
- In the case of micro-roughness the same trends are observed, but within a smaller range, as less grain boundaries come into account: somehow the micro-roughness (~insulated grain surface) is comparable whatever the surface treatment.
- In the case of EP on not annealed samples, although the local surface state seems very smooth, we can reach fairly high roughness when we integrate a large area. Local defects (etching pits) might counterbalance the general smoothness.

#### Conformal equivalent ellipsoid approach

- $a$  and  $b$  parameters are more or less equivalent and are related to the surface of observation, whatever the surface treatment. It means that the grain distribution is uniform, without preferential orientation, as can be expected from a well recrystallized material.
- The  $c$  parameter appears to be the relevant one: it traduces the mean form factor of the defect, and thus gives an indirect idea of the mean field enhancement.
- On annealed samples, large scale ( $9\ \mu\text{m}$ ), we follow the classical roughness parameter:  $\text{FNS} > \text{FNP} > \text{EP}$ ; but at lower scale ( $1\ \mu\text{m}$ ), all the value are close together. This once again traduces the fact that the main difference between those surface treatments arise from the range of grain boundary etching.
- In the case of not annealed samples, we have an inversion between classical roughness parameters and the  $c$  values: apparently, compared to FNS, FNP produces smaller defects, but their mean form factor is higher. This example show the interest of this approach: although roughness parameters seem favourable, this surface state is maybe less interesting from the point of view of field enhancement.

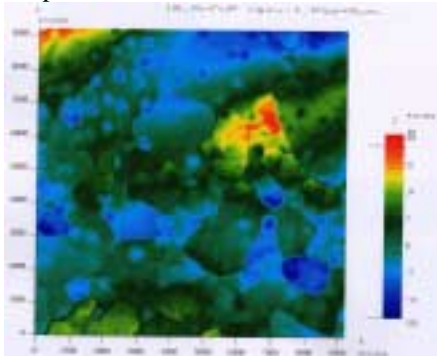


Figure 4: contour line representation for the sample polished with FNS mixture. Grain structure is revealed due to preferential grain boundary etching, and

differential etching rate of individual grains due to their crystalline orientation.

This etching with “step at the grain boundary” allows a macro-graphic visualization of the grain structure of this sample via the representation with contour line (see figure 4).

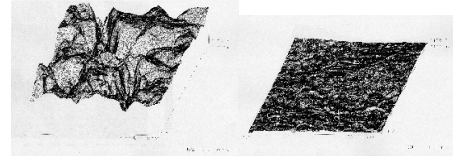


Figure 5: 3D view of annealed samples polished with FNS (left) and FNP (right) (step width  $9\ \mu\text{m}$ , vertical scale  $160\ \mu\text{m}$ ).

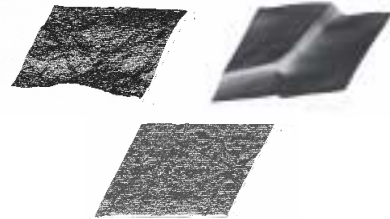


Figure 6: 3D view of annealed samples polished with FNS (top left), FNP (top right) and EP (bottom) (step width  $1\ \mu\text{m}$ , vertical scale  $25\ \mu\text{m}$ ). The surface topography of only one grain exhibits only a light undulation.

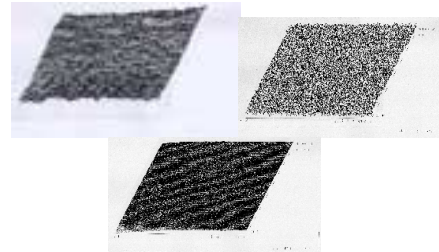


Figure 7: 3D view of not annealed samples polished with FNS (top left), FNP (top right) and EP (bottom) (step width  $9\ \mu\text{m}$ , vertical scale  $160\ \mu\text{m}$ ).

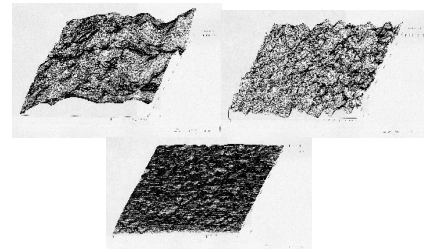


Figure 8: 3D view of not annealed samples polished with FNS (top left), FNP (top right) and EP (bottom) (step width  $1\ \mu\text{m}$ , vertical scale  $25\ \mu\text{m}$ ).

## CONCLUSIONS

We have developed new tools that permit scanning the internal morphology of the surface near the quench area determined by temperature mapping. We observed in the quench area a long and thin prominent grain perpendicular to magnetic field. This is a good candidate

to a possible relation between a surface local irregularity and the quench. Complementary models of local field enhancement should provide realistic figures in order to determine if this effect is important enough to explain the quench.

We have also tried to characterize better the surface state generated by various surface treatments. Conformal equivalent ellipsoids prove to be valuable in the case where the classical roughness parameters tend to be insufficient.

Meanwhile, these studies prove that grain size is the most important parameter that influences the final morphology.

In the case of cavities, where the highest density of current occurs in the heat affected area (i. e. where the largest grains are found), it could be difficult to get a predictable uniform surface state. This could explain why so much dispersion is observed in the EP results for instance.

If these results are confirmed, alternative fabrication schemes without welding could recover a new gain of interest.

## ACKNOWLEDGEMENTS

Authors wish to thank P. Vigier and C. Bataillon from the "Service de la Corrosion et du Comportement des Matériaux dans leur Environnement" for data acquisitions and valuable discussions.

## REFERENCES

- [1] J. Knobloch, et al., "High-Field Q Slope in Superconducting Cavities Due to Magnetic Field Enhancement at Grain Boundaries," 9<sup>th</sup> Workshop on RF Superconductivity, Santa Fe, NM, USA: November 1-5 1999.
- [2] C.Z. Antoine, et al., "Morphological and Chemical studies of Nb Samples after Various Surface Treatment," 9<sup>th</sup> Workshop on RF Superconductivity, Santa Fe, NM, USA: November 1-5 1999.
- [3] N. Bodin, "Description de la topographie des surfaces à l'aide de structures homogénéisées équivalentes conformes," Sciences pour l'ingénieur. 1999, Université de Franche-Comté: Besançon, FRANCE, p. 137.
- [4] C. Roncolato, "personal communication."
- [5] B. Aune, et al., "Superconducting R.F. activities at Saclay," 1988 Linear Accelerator Conference, Newport News, Virginia, USA: October 3-7 1988, p. 432-433.
- [6] S. Berry, C. Antoine, and M. Desmons, "to be published."
- [7] H. Safa, et al., "Nb purification by Ti gettering," 7<sup>th</sup> Workshop on RF superconductivity, Gif-sur-Yvette: October 17-20 1995, p. 649-652.
- [8] We have performed surface profiling on the mechanical microscope of the LECA (CEA Saclay).